Audio Engineering Society

Convention Express Paper 299

Presented at the AES 157th Convention
2024 October 8-10, New York, NY, USA

This Express Paper was selected on the basis of a submitted synopsis that has been peer-reviewed by at least two qualified anonymous reviewers. The complete manuscript was not peer reviewed. This Express Paper has been reproduced from the author's advance manuscript without editing, corrections, or consideration by the Review Board. The AES takes no responsibility for the contents. This paper is available in the AES E-Library (http://www.aes.org/e-lib) all rights reserved. Reproduction of this paper, or any portion thereof, is not permitted without direct permission from the Journal of the Audio Engineering Society.

Generate acoustic responses of virtual microphone arrays from a single set of measured FOA responses. - Apply to multiple sound sources.

Masataka Nakahra[1,2], Toru Kamekawa[3], and Akira Omoto[4,1]

[1] *ONFUTURE Ltd, Tokyo 141-0032 Japan*
[2] *SONA Corporation, Tokyo 164-0013 Japan*
[3] *Tokyo University of the Arts, Tokyo 120-0034 Japan*
[4] *Kyushu University, Fukuoka 815-8540 Japan*

Correspondence should be addressed to Masataka Nakahara (nakahara@onftr.com)

ABSTRACT

We propose a method, V2MA, that virtually generates acoustic responses of any type of microphone array from a single set of FOA responses measured in a target room. An A-format microphone is used for the measurement, but no Ambisonics operation is included in the processing. V2MA is a method based on geometrical acoustics. From a measured FOA response, we calculate instantaneous active sound intensities in the x, y, and z directions, then acoustic information about the virtual sound sources, i.e., the dominant reflections, of the room are detected from them. Although it is desirable to have an A-format microphone place close to the attempted position of the virtual microphone array in the room, it is not a mandatory requirement. Since our method allows to generate SRIRs, spatial room impulse responses, at arbitrary receiver positions in the room by updating the acoustic properties of the virtual sound sources detected at a certain position of the room, an A-format microphone can be placed anywhere you like such as at the one of audience seats. On the other hand, a loudspeaker has to be placed at the source position where a player is assumed to be when virtual recording. Since the positions of virtual sound sources change when a real sound source moves, we need to store a set of virtual sound source data for each assumed real source position. For example, we are required to measure four sets of FOA responses by placing a loudspeaker at four positions, if we would like to generate V2MA responses for a quartet performance. To improve this inconvenient restriction, we developed the technique of updating the positions of the virtual sound sources when a real sound source moves from its original position. Although the technique requires some approximations, it is ascertained that the generated SRIRs provide fine acoustic properties in both physical and auditory aspects.

1 Introduction

We have developed a method to visualize the spatial properties of the acoustic behaviour of a room response, VSV (Virtual Source Visualizer). The method is based on the sound intensity analysis [1], and some unique techniques for detecting virtual sound sources of the room are implemented [2,3].
Recently, it has been reported that the sound particle velocity can be measured using a pair of cardioid microphones, i.e., a figure-of-eight microphone, not only under the characteristic acoustic impedance $z=\rho c$, but also under arbitrary specific acoustic impedances [4]. This means that accurate sound intensities in the X, Y, and Z directions can be obtained from an FOA (First Order Ambisonics) response measured by an A-format microphone. Focusing on this convenience and using the VSV method, we developed a scene-based 3D sampling reverb, VSVerb (Virtual sound Sources reVerb), that restore a 4pi reverberant sound field of a target room from a set of FOA responses [5]. VSVerb is the method based on geometrical acoustics using spatial information about virtual sound sources, like some other previous researches also did [6].

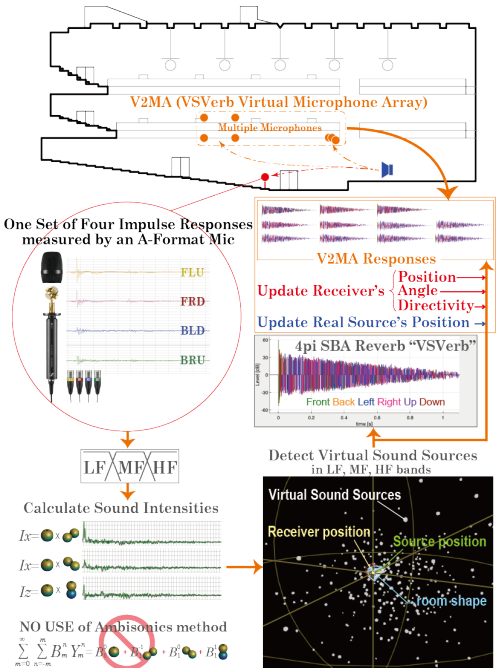


Figure 1. Overview of the V2MA processing flow.

From a room acoustics point of view, VSVerb is one of the correct methods for sound field reproduction. On the other hand, large scale microphone arrays (mikings), are usually preferred for reverb creation of the sound content production. In order to address these needs, we have developed V2MA (VSVerb Virtual Microphone Array), that generates virtual microphone array responses from a set of FOA responses measured by an A-format microphone in a target room [7]. In our previous study, we found that the V2MA works well especially for a point source content such as a solo performance [8]. In this paper, we propose the method of applying V2MA to the multiple positions of sound sources by using only one set of measured FOA responses.

2 V2MA

Figure 1 is for showing the overview of the V2MA, that generates SRIRs (Spatial Room Impulse Responses) of designated microphone arrays virtually from a set of FOA responses measured in a target room. The flow is as follows.

1. Impulse responses are measured in a target room using an A-format microphone, and they are filtered into low, mid, and high frequency bands. Then, filtered responses are converted to FOA signals, W, X, Y, and Z.
2. The instantaneous active sound intensities, Ix=W·X, Iy=W·Y, and Iz=W·Z, are calculated from the Hilbert-transformed FOA signals.
3. Virtual sound sources are detected from the time-averaged instantaneous sound intensities, and their phase characteristics, either + or -, are also estimated. Then, the spatial characteristics of the virtual sound sources at the original microphone position are obtained.
4. Positions of the virtual sound sources are updated with reference to the new receiver positions, i.e., microphone positions of a virtual microphone array. They are obtained by moving the original virtual sources in the opposite direction of the receiver's movement.
5. The positions of the virtual sound sources are updated again when the real source position is moved from the original position, i.e., a measurement loudspeaker position. Details are given in Chapters 3 and 4.
6. The strengths of the virtual sources are updated in inverse proportion to the differences between the distances of the new and original virtual sound source positions to new ones.
7. The strengths of the virtual sound sources are weighted to match the directivities of the microphones in a virtual microphone array.

Omni	1 (no change)	(1)
Figure 8	$\cos(\theta+\theta_0)\cos(\varphi+\varphi_0)$	(2)
Cardioid	$0.500+0.500\cos(\theta+\theta_0)\cos(\varphi+\varphi_0)$	(3)
Super Card.	$0.375+0.625\cos(\theta+\theta_0)\cos(\varphi+\varphi_0)$	(4)
Hyper Card.	$0.250+0.750\cos(\theta+\theta_0)\cos(\varphi+\varphi_0)$	(5)

(θ and φ : elevation and azimuth angles of virtual sources
θ_0 and φ_0 : elevation and azimuth angles of the receiver)

8. Spatial properties of virtual sound sources are translated into time responses, and they are convolved with a source signal in each channel.

3 Virtual Sound Sources

Based on geometrical acoustics, we can consider (A) reflections in a room as (B) the sounds from virtual sound sources that are located outside the room as shown in Figure 2. By translating their spatial properties into the time domain, we can obtain a SRIR. Where, the distances between virtual sound sources and the receiver indicate the arrival times of the reflections, and their amplitudes are given by the strengths of the virtual sound sources.
Although Figure 2 is shown only the first-order reflections that are generated by hitting a wall once, the second-order reflections, i.e., reflections hitting a wall twice, are given by the symmetrical copies of the first-order ones, as shown in Figure 3.

As the reflection order increases, the number of virtual sound sources becomes larger. This means that the higher the order becomes, the farther the area where the virtual sound sources stay, and the larger the number of booths in the area, as shown in Figure 4. Although the shape of the outer and inner boundaries of the areas changes with the shape of the room, the elliptical shapes are given here to simplify this phenomenon. Therefore, we find some virtual sound sources outside their own area in Figure 4.

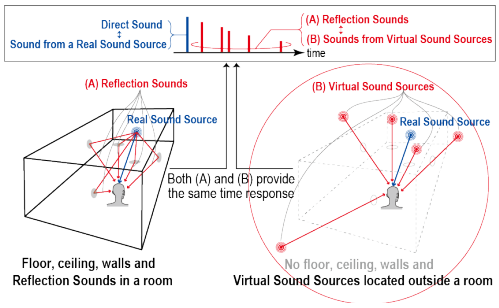


Figure 2. Reflections and Virtual Sound Sources.

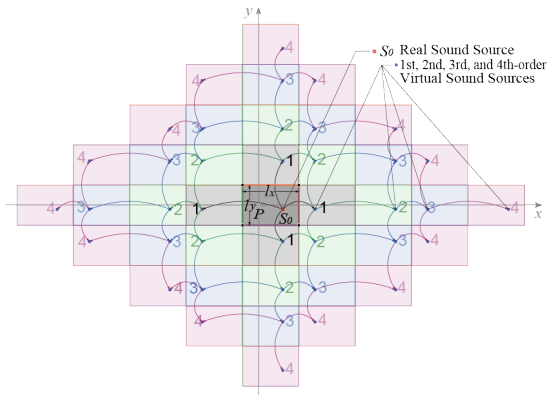


Figure 3. Virtual Sound Sources of 1st-4th order reflections.

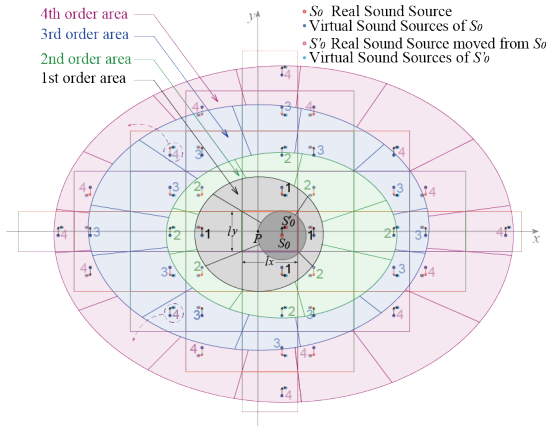


Figure 4. Areas where Virtual Sound Sources are located.

4 Relationship between the movement of the Real Sound source and the positions of the Virtual Sound Sources

The positions of virtual sound sources do not change as long as the real source does not move. Therefore, we can easily regenerate SRIRs at any positions of the receiver by updating the distances of the virtual sound sources to the receiver.

On the other hand, when the real sound source moves, the virtual sound sources will also move. Figure 4 is also for showing how the 1st to 4th-order virtual sound sources move when the real sound source moves from S_0 to S'_0. We can see that the movement of the virtual sound sources follows a certain rule given by their reflection orders and the area where they are located. This suggests that we can predict the movement of virtual sound sources if we can detect their reflection orders and located areas.

In terms of the located areas, the boundaries between neighbouring booths are given by the reflection order and the room dimensions. Figure 5 is for showing the boundaries in the case of the first and second-order virtual sound sources. The boundaries are given by the intersections of the l_x x l_y and l_{xy} x l_z meshes for horizontal and vertical planes, respectively. Where, l_x, l_y, and l_z are the depth, width, and height of the room, and l_{xy} is the cross length when the room floor is cut by the azimuth angle of Φ with the origin point of the real sound source position S_0. In the figure, ($\pm\Delta$x, $\pm\Delta$y) and $\pm\Delta$z indicate the directions of movement of the virtual sound sources when the real sound source moves from S_0 to $S_1 = S_0 + (\Delta x, \Delta y, \Delta z)$. We can see that $\pm$ sings and the orders of the azimuth and elevation areas, $\Phi_{m,i}$ and $\theta_{m,i}$, have a certain rule, and it is different between the reflection orders m.

Figures 6 and 7 illustrate the relationship between the areas, $\Phi_{m,i}$ and $\theta_{m,i}$, and the rules of the $\pm$ signs of the movement of the mth-order virtual sound sources. Tables 1 and 2 are also shown how the areas ($\Phi_{m,i}$, $\theta_{m,i}$) and the directions ($\pm\Delta$x, $\pm\Delta$y, $\pm\Delta$z) are given by the reflection order m.

From Figures 6 and 7 and Tables 1 and 2 we can conclude that even if the real source moves from its original position, new positions of virtual sound sources can be predicted if we allow a room to be approximated as a rectangular shape.

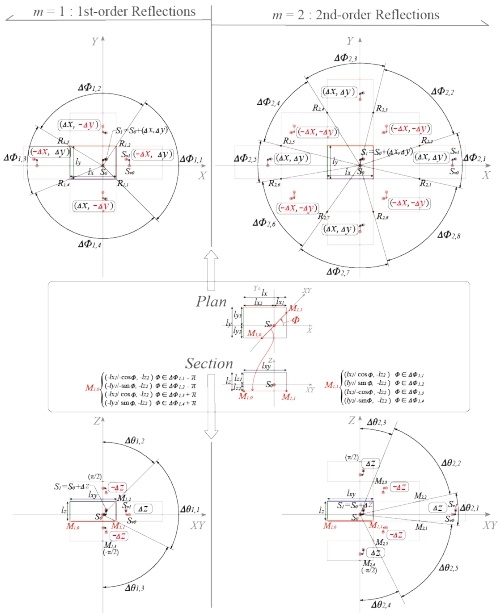


Figure 5. Moving directions (±) of the 1st and 2nd order virtual sound sources when the real sound source moves in a rectangular room of (l_x, l_y, l_z).

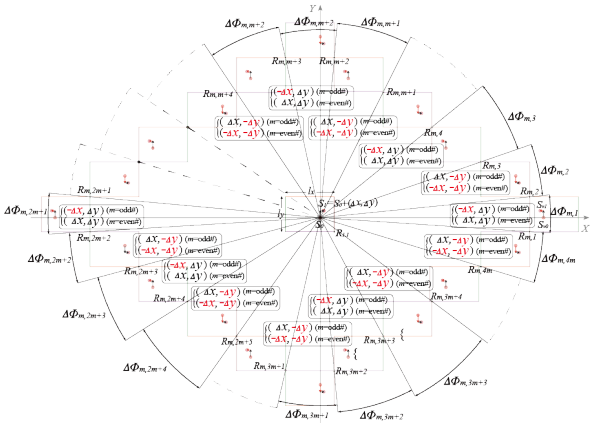


Figure 6. Moving directions (±) of the *m*th-order virtual sound sources on the horizontal plane when the real sound source moves in a rectangular room of (l_x, l_y, l_z).

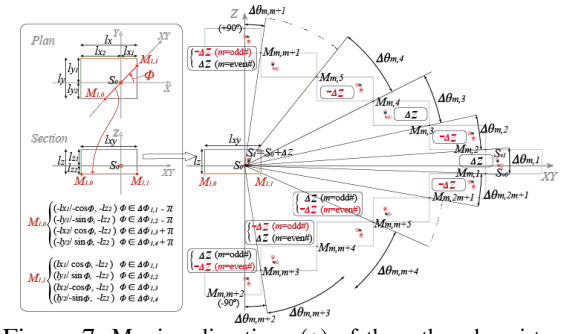


Figure 7. Moving directions (±) of the *m*th-order virtual sound sources on the vertical plane when the real sound source moves in a rectangular room of (l_x, l_y, l_z).

Ref. Order	Area # n		Aperture angle (azimuth) : $\Delta\Phi$m,n Boundary point: Rm,n = R1,1 + (nx lx , ny ly) Rm,n	nx	ny	↔	Rm,n+1	Shifting directions of Virtual Sound Sources m = odd #	m = even #
m	1	$\Delta\Phi$m,1	Rm,1	m-1	0	↔	Rm,2	(-Δx, Δy)	(Δx, Δy)
	2	$\Delta\Phi$m,2	Rm,2	m-1	1	↔	Rm,3	(Δx, -Δy)	(-Δx, -Δy)
	3	$\Delta\Phi$m,3	Rm,3	m-2	2	↔	Rm,4	(-Δx, Δy)	(Δx, Δy)
	⋮		⋮	⋮	⋮		⋮	⋮	⋮
	m+1	$\Delta\Phi$m,m+1	Rm,m+1	⋮	m	↔	Rm,m+2	(Δx, -Δy)	(Δx, Δy)
	m+2	$\Delta\Phi$m,m+2	Rm,m+2	⋮	m	↔	Rm,m+3	(-Δx, Δy)	(-Δx, -Δy)
	m+3	$\Delta\Phi$m,m+3	Rm,m+3	⋮	m-1	↔	Rm,m+4	(Δx, -Δy)	(Δx, Δy)
	⋮		⋮	⋮	⋮		⋮	⋮	⋮
	2m+1	$\Delta\Phi$m,2m+1	Rm,2m+1	-m	1	↔	Rm,2m+2	(-Δx, Δy)	(Δx, Δy)
	2m+2	$\Delta\Phi$m,2m+2	Rm,2m+2	-m	0	↔	Rm,2m+3	(Δx, -Δy)	(-Δx, -Δy)
	2m+3	$\Delta\Phi$m,2m+3	Rm,2m+3	-m+1	-1	↔	Rm,2m+4	(-Δx, Δy)	(Δx, Δy)
	2m+4	$\Delta\Phi$m,2m+4	Rm,2m+4	-m+2	-2	↔	Rm,2m+5	(Δx, -Δy)	(-Δx, -Δy)
	⋮		⋮	⋮	⋮		⋮	⋮	⋮
	3m+1	$\Delta\Phi$m,3m+1	Rm,3m+1	⋮	-m+1	↔	Rm,3m+2	(Δx, -Δy)	(Δx, Δy)
	3m+2	$\Delta\Phi$m,3m+2	Rm,3m+2	⋮	-m+1	↔	Rm,3m+3	(-Δx, Δy)	(-Δx, -Δy)
	3m+3	$\Delta\Phi$m,3m+3	Rm,3m+3	⋮	-m+2	↔	Rm,3m+4	(Δx, -Δy)	(Δx, Δy)
	⋮		⋮	⋮	⋮		⋮	⋮	⋮
	4m	$\Delta\Phi$m,4m	Rm,4m	m-2	-1	↔	Rm,1	(Δx, -Δy)	(-Δx, -Δy)

Table 1. Moving directions of an *m*th-order virtual sound source located in a $\Delta\Phi_{m,\,n}$ azimuth area, when the real source moves for in a rectangular shaped room of (l_x, l_y, l_z).

Ref. Order	Area # n		Aperture angle (elevation) : $\Delta\theta$m,n Boundary point: Mm,n = M1,1 + (nxy lxy , nz lz) Mm,n	nxy	nz	↔	Mm,n+1	Shifting directions of Virtual Sound Sources m = odd #	m = even #
m	1	$\Delta\theta$m,1	Mm,1	m-1	0	↔	Mm,2	Δz	
	2	$\Delta\theta$m,2	Mm,2	m-1	1	↔	Mm,3	-Δz	
	3	$\Delta\theta$m,3	Mm,3	m-2	2	↔	Mm,4	Δz	
	4	$\Delta\theta$m,4	Mm,4	m-3	3	↔	Mm,5	-Δz	
	⋮		⋮	⋮	⋮		⋮	⋮	
	m+1	$\Delta\theta$m,m+1	Mm,m+1	0	m	↔	(+90°)	-Δz	Δz
	m+2	$\Delta\theta$m,m+2	Mm,m+2	(-90°)		↔	Mm,m+3	Δz	-Δz
	m+3	$\Delta\theta$m,m+3	Mm,m+3	0	-m+1	↔	Mm,m+4	-Δz	Δz
	m+4	$\Delta\theta$m,m+4	Mm,m+4	1	-m+2	↔	Mm,m+5	Δz	-Δz
	⋮		⋮	⋮	⋮		⋮	⋮	
	n=2m+1	$\Delta\theta$m,2m+1	Mm,2m+1	m-2	-1	↔	M1,1	-Δz	

Table 2. Moving directions of an *m*th-order virtual sound source located in a $\Delta\theta_{m,\,n}$ elevation area, when the real source moves for in a rectangular shaped room of (l_x, l_y, l_z).

5 Sampling Virtual Sound Sources of a Concert Hall

In order to verify the method proposed in the previous chapter, we generated V2MA responses of a 7.0.4ch microphone array from a set of FOA responses.

Impulse responses were measured with an A-format microphone, Sennheiser's AMBEO VR Mic, at the Fukuoka Symphony Hall. The microphone was placed at one of the audience chairs, and the loudspeaker, Genelec's 8351, was placed on the stage. The microphone and the loudspeaker were placed approximately in the center of the hall, as shown in Figure 8.

Figure 9 is for showing the detected virtual sound sources of the hall in LF (40-500Hz), MF (200-3kHz) and HF (1k-8kHz) bands. Their acoustic properties are also shown in the Table 3.

In the figure, the origin point indicates the receiver position, and the colored dots indicate the virtual sound sources. The distance between the dots and the origin point is proportional to the arrival time of reflection sounds, and the size of the dots indicates the strength of the reflection sounds at the receiver position.

The colors indicate six areas of arrival directions of reflection sounds as follows.

Green	Front	$-45° \le \theta \le 45°$	$-45° \le \varphi \le 45°$
Orange	Back	$-45° \le \theta \le 45°$	$135° \le \varphi \le 180°$ $-180° \le \varphi \le -135°$
Blue	Left	$-45° \le \theta \le 45°$	$45° \le \varphi \le 135°$
Pink	Right	$-45° \le \theta \le 45°$	$-135° \le \varphi \le -45°$
Purple	Up	$45° \le \theta \le 90°$	$-180° \le \varphi \le 180°$
Brown	Down	$-90° \le \theta \le -45°$	$-180° \le \varphi \le 180°$

(θ : elevation angle , φ : azimuth angle)

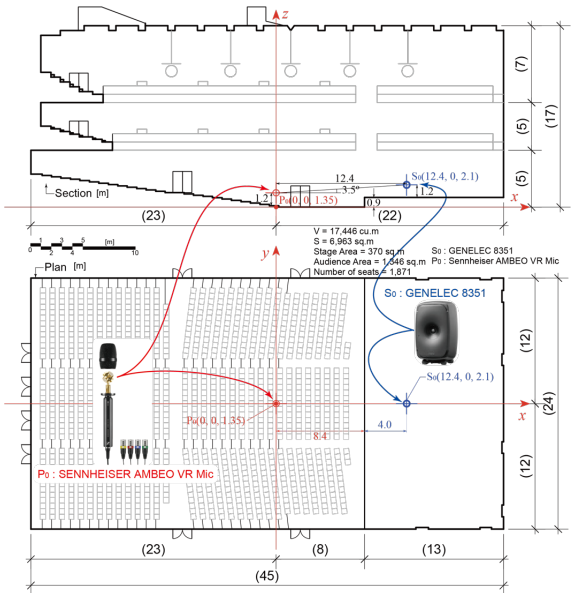


Figure 8. Source (S_0) and receiver (P_0) positions for IR measurement at the Fukuoka Symphony Hall.

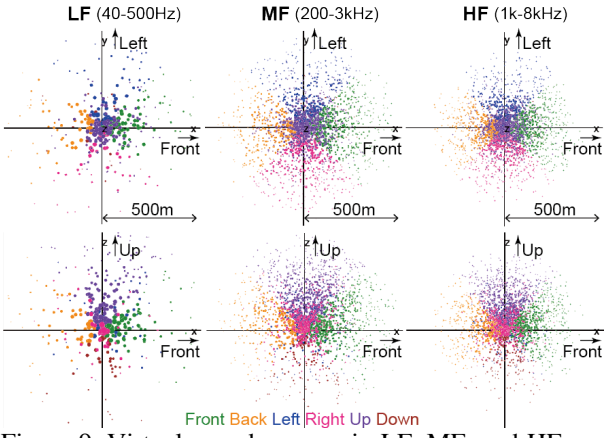


Figure 9. Virtual sound sources in LF, MF, and HF, detected at the P_0 of the Fukuoka Symphony Hall.

	Detected virtual sound sources			Real sound source
	LF 40-500Hz	MF 200-3kHz	HF 1k-8kHz	(Direct sound)
Toal of number	383	2,222	2,631	1
Farthest distance [m]	571.0	505.5	439.0	12.4
Last arrival time [s]	1.66	1.47	1.28	0.036
Smallest level [dB]	-57.1	-58.6	-59.9	0
Reverberation time [s]	2.06	2.37	1.69	-

Table 3. Acoustic properties of the detected virtual sound sources shown in Figure 9.

6 Generate V2MA for the Source Position S_0.

In order to generate eleven SRIRs of a 7.0.4ch virtual microphone array, i.e., V2MA (VSVerb Virtual Microphone Array) responses, we updated the positions and strengths of the virtual sound sources by moving the receiver position, then gave weights of microphone directivities to the strengths of the virtual sound sources.

We assumed to have an Omni-8 array for the L / C / R channels, and a Hamasaki-Cube array for other eight channels, Lss / Rss / Lrs / Rrs / Ltf / Rtf / Ltr / Rtr [9,10]. Figure 10 illustrates the Omni-8 + Hamasaki-Cube array used for the V2MA. We built the array virtually in the Fukuoka Symphony Hall as show in Figure 11.

Figure 12 is for showing the six of the eleven responses of generated V2MA responses in MF (350-2kHz). They show well the acoustical feature of the virtual Omni-8 + Hamasaki-Cube array.

The L contains rich reflections with a strong direct sound captured by an omni-directional microphone. On the other hand, C contains less reflections with a strong direct sound captured by a figure-of-8 microphone. We can know that the Omni-8 array provides a dry C with a reverberant L and R.

As for the lower channels of the Hamasaki-Cube, Lss and Lrs, they provide less direct sounds captured by the figure-of-8 microphones facing to the lateral directions. In terms of the higher channels, Ltf and Ltr, provide a little bit strong direct sound captured by the super cardioid microphones. V2MA responses show that the Hamasaki-Cube provides fine ambience sound with less direct sounds that can avoid from harmful correlation with the L, R and C channels.

The generated V2MA responses were convolved with a dry source using crossover filters at 350Hz and 2kHz for LF, MF, and HF responses, and evaluated to be listened by the authors. The sound impressed with sufficient sound quality and spaciousness of the intended microphone array especially in the case of a solo performance. On the other hand, a quartet performance presented somewhat unnatural spatial impression due to the mono source sound where the various instruments are dubbed into one channel.

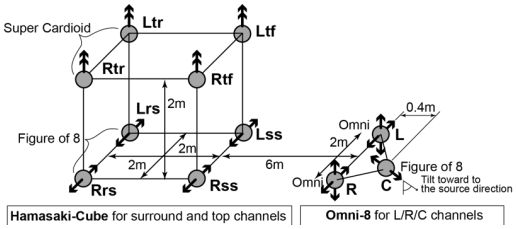


Figure 10. 7.0.4ch virtual microphone array; 3ch Omni-8 + 8ch Hamasaki-Cube [9,10].

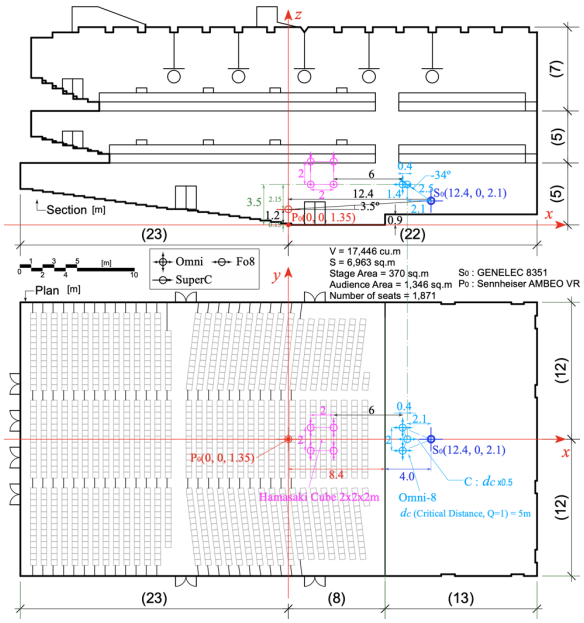


Figure 11. Assumed position of the 7.0.4ch virtual microphone array in the Fukuoka Symphony Hall.

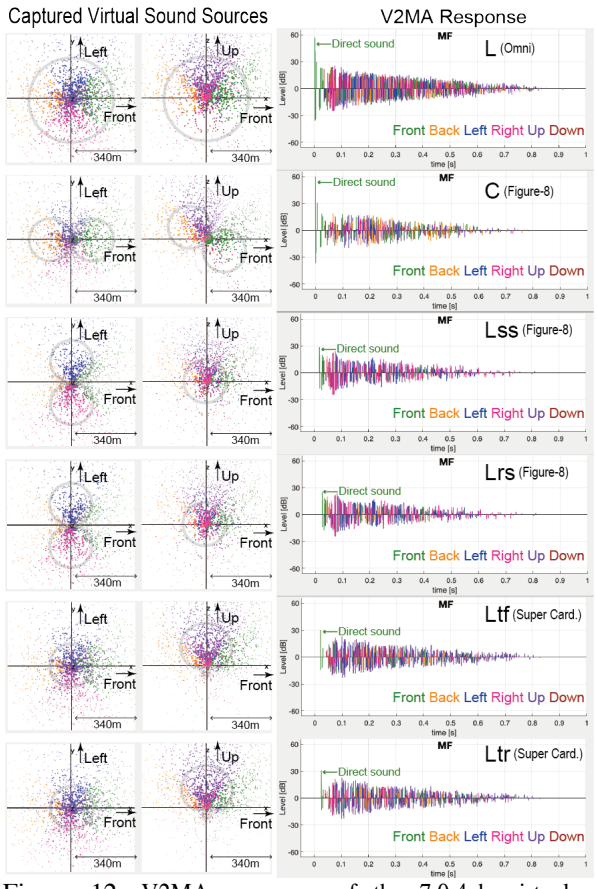


Figure 12. V2MA responses of the 7.0.4ch virtual microphone array in MF (350-2kHz). The source is at S_0.

7 Apply to Multiple Positions of Sound Sources

In order to improve an unnatural spatial impression played back by the mono source where the multiple sound instruments are dubbed, we generated four different V2MA responses for a string quartet performance.

As we discussed in Chapter 4, the reflection order m has to be estimated to update the positions of the virtual sound sources to match the new real source position. If we allow the inner and outer boundaries of the virtual sound source areas to be simplified as a spherical surface with a radius of $l_d + m \cdot l_{vi}$, we can estimate the reflection order m from the mean free path l_m as shown in equation (6).

$$m = (l_{vi} - l_d) / l_m \quad (6)$$

- m reflection order of a virtual sound source
- l_{vi} distance between a virtual sound source and the original receiver position [m]
- l_d distance between a real sound source and the original receiver position [m]
- l_m mean free path [m]

According to a recent study of statistical acoustics [11], the cumulative summation of virtual sound sources N over time t is described by three parameters; mean free path l_m, reflection dimension n, and sound speed c as shown in equation (7).

$$N = (c\, t / l_m)^{n} \quad (7)$$

- N cumulative summation of virtual sound sources
- l_m mean free path [m]
- n reflection dimension $\in (1, 3]$
- c sound speed [m/s]
- t time since the direct sound arrived [m/s]

Although it is widely known that the mean free path l_m is calculated from the room dimensions, e.g., $l_m = 4V/S$ [m] in the case of n=3, (7) suggests that the realistic l_m can be estimated not from the theoretical value but from N of the detected virtual sound sources. To obtain a realistic value for l_m, we estimate it from the number of detected virtual sound sources.

Table 4 is shown the estimated results of l_m and n in the low, mid, and high frequency bands from the N of the virtual sound sources detected at the Fukuoka Symphony Hall.

If we consider the floor of the hall as a whole sound absorbing surface, the reflection dimension n of the hall is regarded as an approximate 2, and the theoretical value of l_m is calculated to be 24.39m. On the other hand, the estimated values of (n, l_m) are (1.09, 2.07m), (1.31, 1.19m), and (1.30, 0.74m) in LF, MF,

and HF bands, respectively. In the theory, the reflection dimension n is usually given by an integer value, 1 (1D), 2 (2D), or 3 (3D), but the estimated n shows that the reflection dimension n of the real world seems to be a decimal value that varies with frequency.

Figure 13 is shown the comparison of N-curves. In the figure, dark-colored curves indicate the detected values, and light-colored curves indicate the calculated values from the estimated l_m and n. Since no significant differences can be found between detected and calculated values, we decided to use the estimated l_m, listed in Table 4, to calculate the reflection order m for each virtual sound source.

With reference to Tables 1, 2, 4, and the equation (6), we updated the positions of virtual sound sources to meet the new real source positions, S_1, S_2, S_3, and S_4 in Figure 14.

The L and R responses of the updated V2MA are shown in the Figures 15 and 16. They are shown the positions of the virtual sound sources and their time responses with focusing on the early part of the response. Figure 17 is also for showing the envelopes of the early part of the responses between the original position of the real source, S_0 (center), and two of the new positions, S_1 (left) and S_4 (right). They show appropriate time shifts and amplitude changes of the direct sounds between channels, and also show that the different reflections are given by the different source positions.

The updated V2MA responses for four source positions, S_1, S_2, S_3, and S_4, were convolved with Vn1, Vn2, Va, and Vc, respectively, and evaluated for listening. The authors' listening impressions confirmed a significant improvement in the stereophonic image of the instruments.

	Estimated values from the measurement			Theoretical values from the room dimensions $(l_x, l_y, l_z) = (45\text{m}, 24\text{m}, 17\text{m})$
	LF 40-500Hz	MF 200-3kHz	HF 1k-8kHz	
Reflection dimension n	1.09	1.31	1.30	(assumed to be) 2
Mean free path [m] l_m	2.07	1.19	0.74	24.39 $l_m = \pi S_{xy} / l_{xy}$ $S_{xy} = l_x \cdot l_y$, $lxy = 2(l_x + l_y)$

Table 4. Mean free path l_m and the reflection order n of the Fukuoka Symphony Hall estimated from the number N of the detected virtual sound sources.

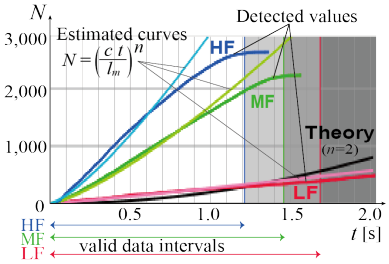


Figure 13. Curves of the number N of the detected virtual sound sources and the regression curves calculated from the estimated l_m and n.

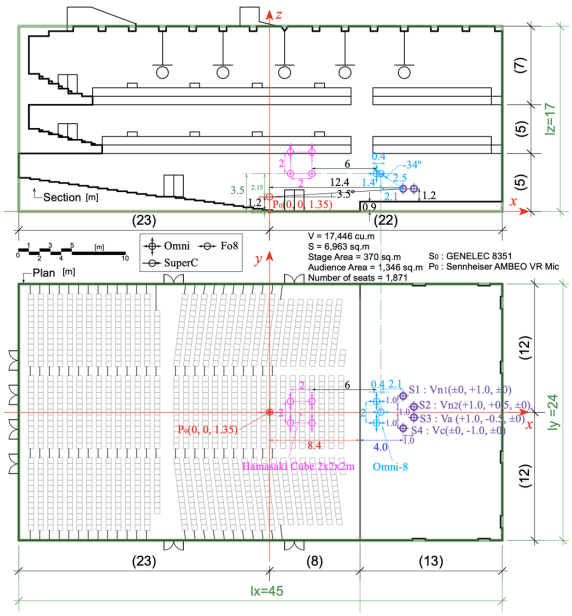


Figure 14. Four new source positions S_1 - S_4 for virtual recording via the 7.0.4ch virtual microphone array.

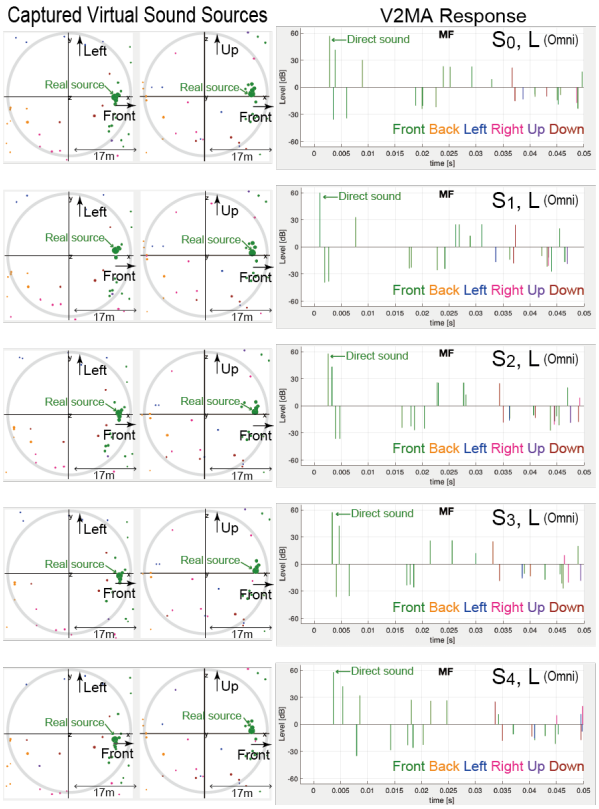


Figure 15. Early part of the Lch responses in MF (350-2kHz) of the 7.0.4ch virtual microphone array, when the source is at S_0, S_1, S_2, S_3, and S_4.

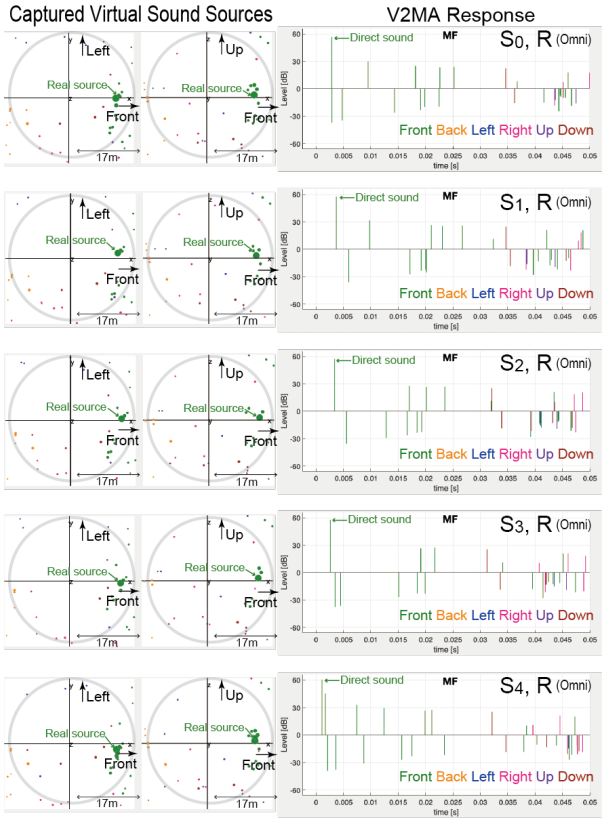


Figure 16. Early part of the Rch responses in MF (350-2kHz) of the 7.0.4ch virtual microphone array, when the source is at S_0, S_1, S_2, S_3, and S_4.

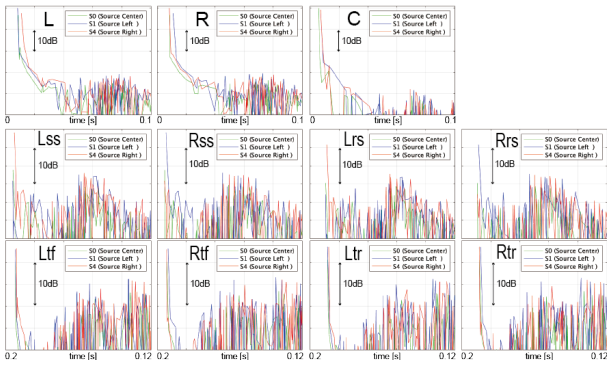


Figure 17. Comparison of the early part of the envelopes of the 7.0.4ch virtual microphone array's responses in MF (350-2kHz) between source positions; S_0 (center), S_1 (left), and S_4 (right).

8 Conclusions

We proposed the method of applying the movement of the real source position to V2MA. By simplifying a room as a rectangular shape, it is ascertained that the positions of virtual sound sources can be updated to match the new real source position, and the stereophonic image of the source sound is significantly improved. Regarding the estimated values of l_m from the number of detected virtual sources, large differences from the theoretical value were found.

The authors intend to further investigate the accuracy of the l_m estimation, and plan to conduct objective and subjective evaluations of the updated virtual sound sources using the proposed method.

References

[1] R. W. Guy and A. Abdou, "A measurement system and method to investigate the directional characteristics of sound fields in enclosures," Noise Control Eng. J., 41, 8–18 (1994)

[2] M. Nakahara, A. Omoto, and Y. Nagatomo, "Accurate extraction of dominant reflections from measured sound intensity responses in a room," eB, AES 142nd Convention, Berlin (2017)

[3] M. Nakahara, Y. Nagatomo, and A. Omoto, "Development of a 4-pi sampling reverberator, VSVerb. -Phase Detection," eB, AES 148th Convention, Virtual Vienna (2020)

[4] T. Hanyu and K. Hoshi, "Method for analyzing sound pressure and sound particle velocity using cardioid microphones," Acoust. Sci. & Tech. 45, 2 (2024)

[5] M. Nakahara, Y. Nagatomo and A. Omoto, "VSVerb, a practical method of reproducing spatial reverberation from virtual sound sources captured in a room," Proc, 24th ICA, Gyeongju (2022)

[6] T. Hanyu, "A new algorithm for generating realistic three-dimensional reverberation based on image sound source distribution in consideration of room shape complexity," Proc, AES 133rd Convention, San Francisco (2012)

[7] M. Nakahara, A. Omoto, and Y. Nagatomo, "Virtual 3D microphone arrays by virtual sound sources detected from an FOA response," Proc, AES International Conference on Spatial & Immersive Audio, Huddersfield (2023)

[8] M. Nakahara, T. Kamekawa and A. Omoto, "Immersive recording using a virtual microphone array generated from an FOA response," Proc, AES 156th Convention, Madrid (2024)

[9] T. Kamekawa, "Impression Differences by Placement of Front and Rear Microphones for Multichannel Stereo Recording," Proc, AES 118th Convention, Barcelona (2005)

[10] K. Hamasaki, "Microphone Techniques for Natural Music Recording," Master Class, AES 152nd Convention, Hague / Online (2022)

[11] T. Hanyu and K. Hoshi, "Relationship between reflected sound density and mean free path in consideration of room shape complexity," Acoust. Sci. & Tech. 33, 3 (2012)